Proceedings of the ASME 2012 Summer Heat Transfer Conference
HT2012
July 8-12, 2012, Rio Grande, Puerto Rico

HT2012-58038

MELTING, VAPORIZATION AND RESOLIDIFICATION IN A THIN GOLD FILM IRRADIATED BY MULTIPLE FEMTOSECOND LASER PULSES

Yijin Mao, Yuwen Zhang, and J.K. Chen
Department of Mechanical and Aerospace Engineering,
University of Missouri
Columbia, MO, 65211, USA
Email: zhangyu@missouri.edu

ABSTRACT

Melting, vaporization and resolidification in a gold thin film subject to multiple femtosecond laser pulses are numerically studied in the framework of the two-temperature model. The solid-liquid phase change is modeled using kinetics controlled model that allows the interfacial temperature deviates from the melting point. The kinetics controlled model also allows superheating in the solid phase during melting and undercooling in the liquid phase during resolidification. Superheating of the liquid phase caused by nonequilibrium evaporation of the liquid phase is modeled by adopting the wave hypothesis, instead of Clausius-Clapeyron equation. Melting depth, ablation depth, and maximum temperature in both liquid and solid are investigated and the result is compared with that from Clausius-Clapeyron equation based vaporization model. The vaporization wave model predicts a much higher vaporization speed which leads to a deeper ablation depth. The relationship between laser processing parameters, including pulse separation time and pulse number, and phase change effect are also studied. It is found that longer separation time and larger pulse number will cause lower maximum temperature within the gold film, as well as lower depths of melting and ablation.

INTRODUCTION

Phase changes widely occur in laser-based advanced manufacturing and material processing, like laser drilling, cutting, cladding, welding, surface treatment, and Direct Metal Selective Laser Sintering (DMSLS). Various numerical works have been carried out to study phase change processes, including melting, evaporation and resolidification induced by laser pulse irradiation, including continuum model [1, 2], molecular dynamics model [3], and hybrid atomistic continuum model [4]. Pulsed laser, due to its high efficiency and high power density, has drawn more and more attention recently. When the laser duration time is around 10^{-13} s, which is close to the mean free time between collision of electrons in metals, nonequilibrium between electrons and the lattice becomes significant; therefore, classical heat transfer model cannot be applied to analyze physical phenomena. Two-temperature model, which was originally proposed by Anisimov et al. [5], and then rigorously derived by Qiu and Tien [6] based on the Boltzmann equation, is widely accepted for simulating femtosecond laser-material interactions. It could also be used to derive the dual-phase-lag model which consider lagging behavior of different energy carriers [7, 8] if the material thermophysical properties are considered to be constants. Jiang and Tsai extended the existing two-temperature model to high electron temperature with full-run quantum treatments to calculate the significant temperature dependent material properties [9]. Chen et al., [10] proposed a semi-classical two-step heating model, which takes electron drifting effect into account, to investigate thermal transport in metals caused by ultra-short laser irradiation.

Huang et al. [11] developed a model that can track the evolution of both solid-liquid and liquid-vapor interfaces in a thin metal film under multiple ultra-short laser pulses interaction by employing Clausius-Clapeyron equation based on ideal gas and thermal equilibrium assumptions. Huang et al. [1] also simulate the non-equilibrium phase change process under single ultra-short laser pulse interaction by introducing wave hypothesis model which was qualitatively demonstrated by the current and voltage curves measured during expanding metal wires [12]. In this paper, simulations of ultrafast phase change process under multiple ultra-short pulses interaction will be carried out, with wave hypothesis model adopted to describe the vaporization process. The rapid solid-liquid-vapor phase change in a free standing gold film induced by irradiation

of multiple femtosecond laser pulses will be numerically studied. The relationship between results, including melting depth, ablation depth, and maximum temperature in both liquid and solid, and the effects from laser fluence and separation time between two pulses are investigated. The new results will be compared with that from Clausius-Clapeyron equation based vaporization model.

NOMENCLATURE

Be	Coefficient for electron heat capacity (J/m^3-K^2)
C	heat capacity (J/m^3-K)
c	speed of sound (m/s)
c_p	specific heat (J/kg-K)
G	electron-lattice coupling factor (W/m^3-K)
h	latent heat of phase change (J/kg)
J	laser fluence (J/m^2)
k	thermal conductivity (W/m-K)
L	thickness of the metal film (m)
M	molar mass (kg/kmol)
p	pressure (Pa)
q''	heat flux (W/m^2)
R	reflectivity
R_g	specific gas constant (J/kg-K)
R_u	universal gas constant (J/kg-K)
s	interfacial location (m)
S	intensity of the internal heat source (W/m^3)
t	time (s)
t_p	pulse width (s)
T	temperature (K)
T_F	Fermi temperature (K)
T_m	melting point (K)
u	interfacial velocity (m/s)
J_i	single pulse fluence (J/m^2)
F_{req}	repetition rate (Hz)
T_{sep}	separation time (s)
V_0	interfacial velocity factor (m/s)
x	coordinate (m)
Greek Symbols	
δ	optical penetration depth (m)
δ_b	ballistic range (m)
ε	total emissivity
ρ	density (kg/m^3)
σ	Stefan-Boltzmann constant (W/m^2-K^4)
Superscripts	
0	last time step
Subscripts	
e	electron
i	initial condition
l	lattice
ℓ	liquid
ℓv	liquid-vapor interface
R	thermal radiation
s	solid
$s\ell$	solid-liquid interface
∞	ambient environment

Physical Model

The physical model of the problem under consideration is illustrated in Fig. 1. Multiple temporal Gaussian laser pulses are irradiated on the left side of a free-standing gold film, whose thickness is L and the initial temperature uniformly equals to T_i. Parameters t_p and J, represents the pulse duration (full width at half maximum; *FWHM*) and fluence of the laser beam, respectively. Due to the fact that L is quite small comparing with the radius of the laser beam, the current problem is approximated to be one dimensional.

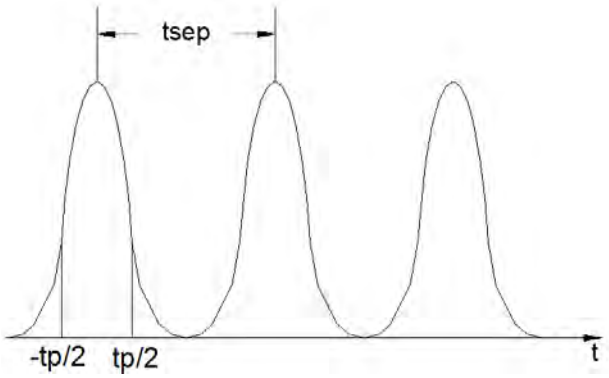

(a) multiple laser pulses

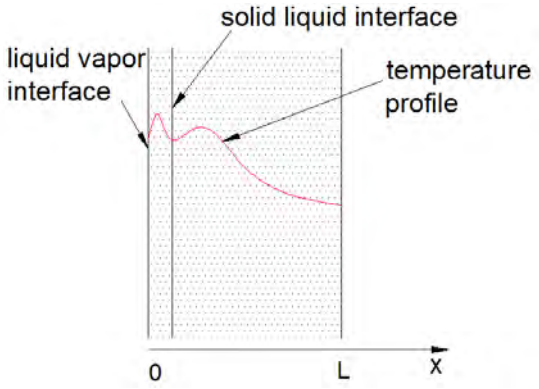

(b) temperature profile within gold film

Fig.1 Physical model

In the two-temperature model, the temperatures of electrons and lattice are calculated separately and coupled by a term proportional to temperature difference between electrons and lattice. Since the duration of laser pulses to be considered is 100 *fs*, which means they are longer than the relaxation time of electrons in gold (~10 *fs*) [13], the heat conductions in both electron and lattice are assumed to be parabolic [14]. The energy equations of the free electrons and lattice are:

$$C_e \frac{\partial T_e}{\partial t} = \frac{\partial}{\partial x}\left(k_e \frac{\partial T_e}{\partial x}\right) - G(T_e - T_l) + S \quad (1)$$

$$C_l \frac{\partial T_l}{\partial t} = \frac{\partial}{\partial x}\left(k_l \frac{\partial T_l}{\partial x}\right) + G(T_e - T_l) \quad (2)$$

The heat capacity of electron, C_e, is approximated by formulas based on the reference [15],

$$C_e = \begin{cases} B_e T_e, & T_e < T_F/\pi^2 \\ 2B_e T_e/3 + C_e^{'}/3, & T_F/\pi^2 \le T_e < 3T_F/\pi^2 \\ Nk_B + C_e^{'}/3, & 3T_F/\pi^2 \le T_e < T_F \\ 3Nk_B/2, & T_e \ge T_F \end{cases} \quad (3)$$

where,

$$C_e^{'} = B_e T_F/\pi^2 + \frac{3Nk_B/2 - B_e T_F/\pi^2}{T_F - T_F/\pi^2}(T_e - T_F/\pi^2) \quad (4)$$

The thermal conductivity of electrons, k_e, can be calculated by [16]:

$$k_e = \chi \frac{(\vartheta_e^2 + 0.16)^{5/4}(\vartheta_e^2 + 0.44)\vartheta_e}{(\vartheta_e^2 + 0.092)^{1/2}(\vartheta_e^2 + \eta\vartheta_l)} \quad (5)$$

where $\vartheta_e = T_e/T_F$ and $\vartheta_l = T_l/T_F$. For gold, this equation is still valid even if the electron temperature is comparable to the Fermi temperature, which is 6.42×10^4 *K*. Indeed, when $\vartheta_e << 1$, eq. (5) could be reduced to:

$$k_e = k_{eq}\left(\frac{T_e}{T_l}\right) \quad (6)$$

In eqs. (1) and (2), *G* is the electron-lattice coupling factor, which accounts for the heat transfer from hot electrons to relatively cold lattice through collisions. Since *G* value is temperature-dependent, the following phenomenological equation is adopted in the current work [17]:

$$G = G_{RT}\left[\frac{A_e}{B_l}(T_e + T_l) + 1\right] \quad (7)$$

Due to the fact that the electrons are more likely to collide with atoms in liquid phase than the atoms in solid crystals, the *G* value in the liquid phase is taken to be 20% higher than that of the solid [15].

The laser irradiation is considered as a source term *S* in energy equation for electron [11].

$$S = \sum_{j=1}^{N} 0.94 J_i \frac{1-R}{t_p(\delta+\delta_b)[1-e^{-L/(\delta+\delta_b)}]} \times e^{\left[-\frac{x}{(\delta+\delta_b)} - 2.77\left(\frac{t-t_i}{t_p}\right)^2\right]} \quad (8)$$

where *R* is the reflectivity of the thin film, δ is the optical penetration depth, δ_b is for the ballistic depth, and term 1- $e^{-L/(\delta+\delta b)}$ is used to correct the film-thickness effect, t_i represents the time when a laser pulse will be injected. The ballistic motion effect from hot electrons is accounted in eq. (8). Wellershoff et al. [18] demonstrated that the inclusion of ballistic depth could lead to a better simulation results to fit the experiment data, because the incident energy caused by the ballistic motion will be brought into a much deeper place of the film.

For metals at thermal equilibrium state, its thermal conductivity, k_{eq}, is the sum of the electron thermal conductivity, k_e and the lattice thermal conductivity, k_l. In most cases k_e dominates k_{eq} because free electrons contribute to the majority part of heat conduction. For gold, k_l is usually taken to be 1% of k_{eq}, [19], i.e.,

$$k_l = 0.01 k_{eq} \quad (9)$$

All the simulations start from $t = -2t_p$ and a uniform temperature distribution are given as initial condition:

$$T_e(x, -2t_p) = T_l(x, -2t_p) = T_i \quad (10)$$

The adiabatic condition is applied to the right side which has no laser irradiation, while heat loss caused by radiation on the left side of the film is considered.

$$\left.\frac{\partial T_e}{\partial x}\right|_{x=0} = \left.\frac{\partial T_e}{\partial x}\right|_{x=L} = \left.\frac{\partial T_l}{\partial x}\right|_{x=L} = 0 \quad (11)$$

$$\left. q^{''}\right|_{x=0} = \sigma\varepsilon(T_{sur}^4 - T_\infty^4) \quad (12)$$

where T_{sur} equals to the lattice temperature at $x = 0$ before evaporation takes place. After evaporation starts, T_{sur} will be the temperature value at the liquid-vapor interface.

During rapid melting/solidification processes, nucleation dynamics dominates the velocity of the interface instead by energy balance [20]. For short-pulse laser melting of gold, since the energy balance equation at liquid and solid interface [15] is:

$$k_{l,s}\frac{\partial T_{l,s}}{\partial x} - k_{l,\ell}\frac{\partial T_{l,\ell}}{\partial x} = \rho_\ell h_m u_s, x = s(t) \quad (13)$$

Thus, the velocity of the solid-liquid interface can be expressed as:

$$u_{s\ell} = V_0\left[1 - e^{\left(-\frac{h_m}{R_g}\frac{T_{l,I}-T_m}{T_m}\right)}\right] \quad (14)$$

where V_0 is the maximum interface velocity, R_g is the universal gas constant for the metal, and $T_{l,I}$ is the solid-liquid interfacial temperature. The interfacial temperature, $T_{l,I}$, is higher than melting point, T_m, during melting process and it will be lower during solidification.

To locate the liquid-vapor interface, energy balance and kinetics laws of evaporation will be applied. The energy balance at the liquid-vapor interface can be expressed as:

$$\rho h_{\ell v} u_{\ell v} + \sigma\varepsilon(T_{lv}^4 - T_\infty^4) = k_l\frac{\partial T_l}{\partial x} \quad (15)$$

where h_{lv} is the latent heat of evaporation, u_{lv} is the velocity of the liquid-vapor interface, T_{lv} is the liquid-vapor interfacial temperature. If interface velocity is known, eq. (15) can be applied to calculate the interfacial temperature T_{lv}.

In order to capture interface of vaporization, one option is to use Clausius-Clapeyron equation that describe the slope of saturation pressure-temperature curve; it is limited by the assumptions of ideal gas and thermal equilibrium. Since vaporization take place during ultrafast non-equilibrium stage, wave model is used to characterize the vaporization process. Bennett, who first raised the vaporization wave model, has already demonstrated this theory during his study on the kinetics of volume vaporization in electrically exploded wires [12]. The velocity of the dynamic evaporation process is limited by the characteristic speed of sound of the two-phase region of the fluid, since the local velocity of sound limits the propagation speed of an expansion wave's front according to shock wave theory [21]. The chosen speed is that of the coexistence side of the liquidus line, which is the low volume boundary of the two phase region. The current and voltage curves measured during expanding metal wires has qualitatively demonstrated vaporization wave hypothesis. The numerical solution based on this hypothesis could well explain pulse shapes produced under different experiment conditions. A thermodynamic model was also developed to make computerized calculation possible. Indeed, the theoretical

prediction agreed well with the results deduced from experiments on Al, Cu and Au. For copper, the wave speed wires ranged from 0 m/s to 300 m/s when they were heated rapidly from the solid state up to the critical temperature with heating rate in the order of $10^9 K/s$. This hypothesis was first considered as vaporization model in the simulation of single laser pulse interaction with the thin gold film by Huang et al. [1].

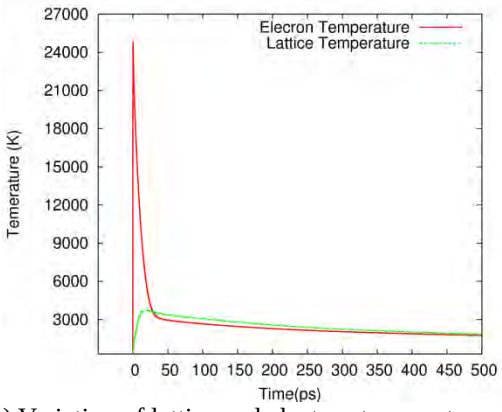

(a) Variation of lattice and electron temperature at surface

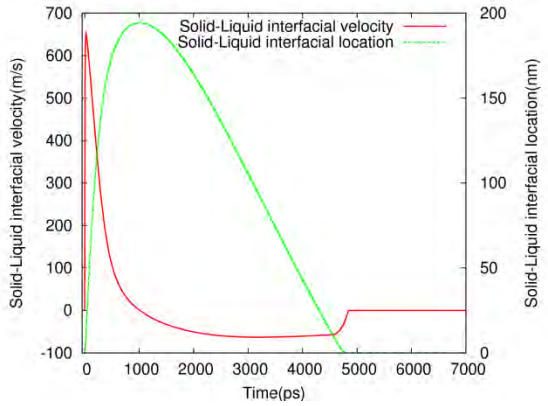

(b) Solid-liquid interfacial velocity and location

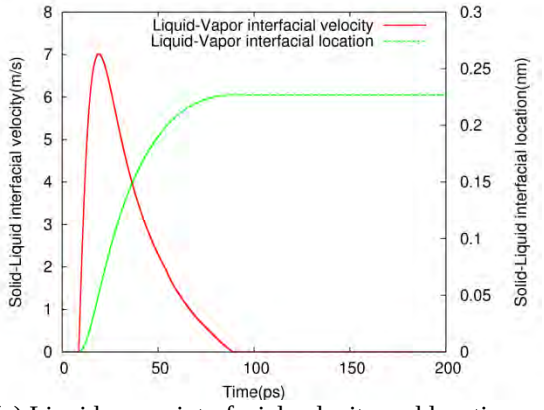

(c) Liquid-vapor interfacial velocity and location

Fig.2 Irradiation by a 0.6J/cm^2 single pulse

In this work, the wave speed will be calculated based on the equation of state, since the experimental data is lacking. The detailed explanation of the method is well given in reference [1]. After the relationship between liquid-vapor interface velocity and surface temperature is established, it will be used to obtain vaporization speed at corresponding surface temperature in order to improve computational efficiency.

Result s and discussion

The gold film thickness for all cases is fixed at 1 μm in this work. The initial temperature T_0 is set to be 300 K. The laser pulse duration time is 100 fs. The thermophysical and optical properties can be found in [22].

1 Single pulse

The result from a single pulse (J = 0.6 J/cm^2) is selected to benchmark the melting, evaporation and resolidification processes which are caused by the multiple pulses. The results, including electron and lattice temperature evolution at the film surface, variation of the solid and liquid interfacial velocity and location as well as the interfacial velocity and location of liquid and vapor, are given in reference [1]. Variation of lattice and

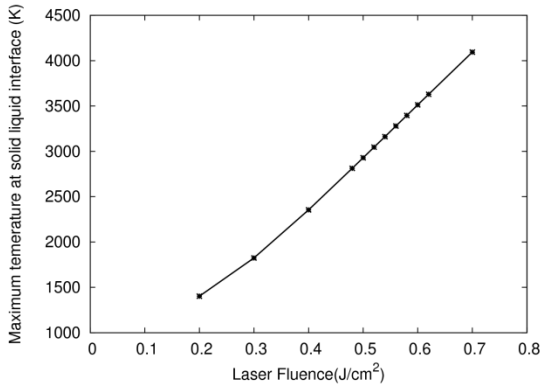

(a) Dependency of maximum solid-liquid interfacial temperature on laser fluence

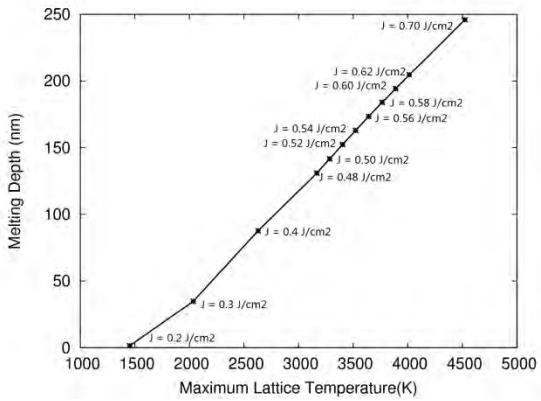

(b) Dependence of melting depth on maximum lattice temperature

Fig. 3 The relationship between laser fluence, maximum lattice temperature and melting depth with single pulses.

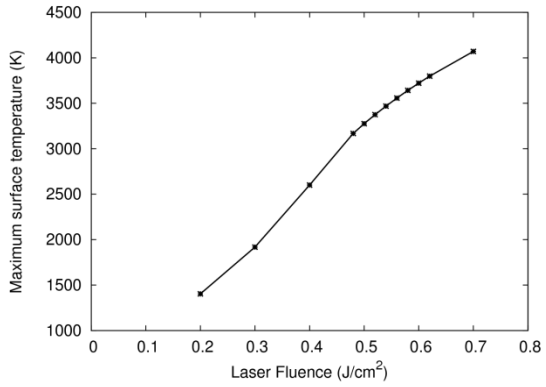

(a) Dependence of maximum surface temperature on laser fluence

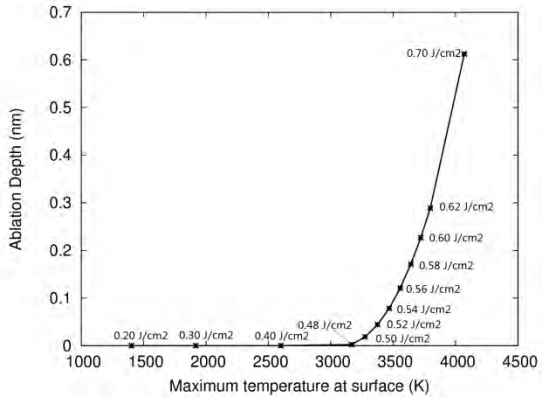

(b) Dependence of ablation depth on maximum temperature with single pulse

Fig. 4 The relationship between the laser fluence, maximum surface temperature and ablation depth with single pulse.

electron temperature at film surface, velocity and location at interface between solid and liquid and velocity and location at interface between liquid and vapor are given in Fig.2 (a), (b), (c). Since melting process is controlled by nucleation dynamics equation, changes in evaporation model will not affect the result at the interface of liquid and solid until ablation depth is larger enough to impact material properties due to its phase dependency; this explains the result shown in Fig. 2 (a), (b), and (c) are the same to that in the reference [1]. However, the maximum temperature within the film will be affected by the changes in vaporization model.

Figure 3 (a) and (b) give the relationship between maximum temperature at solid-liquid interface and laser fluence, and the relationship between maximum lattice temperature and melting depth respectively. As shown in Fig. 3 (a), the maximum temperature at the solid-liquid interface is higher than the melting point, and they are increasing as the laser fluence goes from 0.2 J/cm^2 to 0.7 J/cm^2. The linear response is especially obvious when the laser flucene value ranges from 0.3 J/cm^2 to 0.7 J/cm^2, which means that the maximum temperature is predicable if the fluence is within this range and if the temperature is lower than $0.9T_c$[1]. Figure 3 (b) shows the relationship between maximum lattice temperature and maximum melting depth under different laser fluence values. The linear relationship is quite obvious, especially, when laser intensity varies from 0.2 J/cm^2 to 0.7 J/cm^2.Figure 4 (a) shows the variation of the maximum surface temperature with the laser fluence. It can be seen that the slope of the maximum surface temperature versus laser intensity slightly decreases when laser flucene is higher than 0.48 J/cm^2. A well linear relation between them still exists within several discretized laser intensity ranges, like from 0.2 J/cm^2 to 0.48 J/cm^2 and from 0.48 J/cm^2 to 0.62 J/cm^2. Figure 4 (b) gives the relationship between maximum surface temperature and ablation depth. Evaporation does not occur for the cases with laser fluence below 0.48 J/cm^2. Cases with higher laser intensity lead to deeper ablation with a polynomial-like relation. In comparison with melting depth, the ablation depth is much smaller, but it is much higher than that obtained from Clausius-Clapeyron equation based model.

In the following discussion, Figs. 3(b) and 4(b) will be used as the bases of the comparison between multiple pulses and single pulse. If the resultant point of a multiple pulses irradiation is located in the upper part of Fig 3. (b), it means multiple pulses will obtain deeper melting with the same maximum temperature, and vice-versa. Similarly, if a point of multiple pulses located in the upper part of Fig. 4 (b) means multiple pulses will lead to deeper ablation depth with the same maximum temperature. In other words, it means that multiple pulses can achieve the same ablation depth with lower temperature, which is desirable in laser-material processing.

2 Two pulses

Two consecutive pulses with same laser intensity ($J_1 = J_2 =$ 0.3 J/cm^2) and a separation time of Δt = 280 ps are studied first. Figure 5 (a) shows a typical evolution of electron and lattice temperature at the surface of the gold film. It can be seen that the electron temperature shoots up to around 16,700 K within 0.11 ps, and lattice temperature reach to its first peak point (1,916 K) at around 18ps. For the electron temperature, the second highest temperature is reached at around 16, 300 K, which is lower than the first peak, at around 280.13 ps. The second lattice temperature peak reached to around 3,200 K, which is much higher than the first one due to the utilization of residual thermal energy deposited by the first pulse, at around 297.66 ps. Figure 5 (b) shows that two peaks appear during the evolutions of the interfacial velocity and location of solid-liquid interface. However, as shown in Fig. 5 (c), there is only one peak in liquid-vapor interfacial velocity, which is caused by the second pulse. The maximum surface temperature raised by a single pulse of 0.3 J/cm^2 is lower than threshold value for evaporation. Utilizing the resultant thermal energy from the first pulse, the second pulse can easily reach to the threshold value. Again, the maximum evaporation velocity is higher than that from old model. For the maximum ablation depth, the value is also much higher.

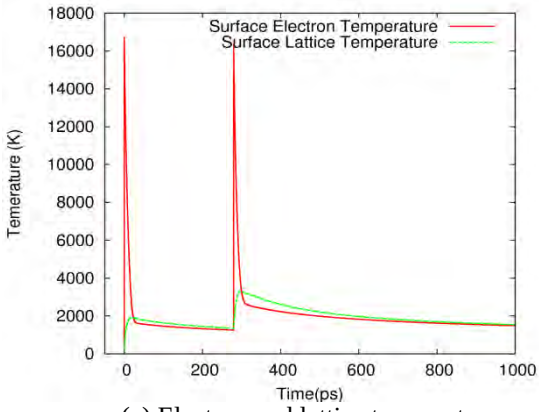

(a) Electron and lattice temperature

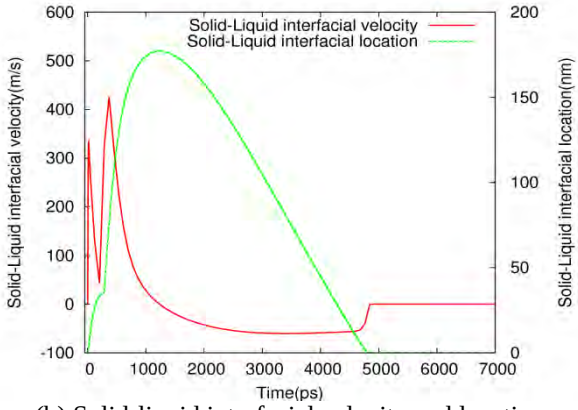

(b) Solid-liquid interfacial velocity and location

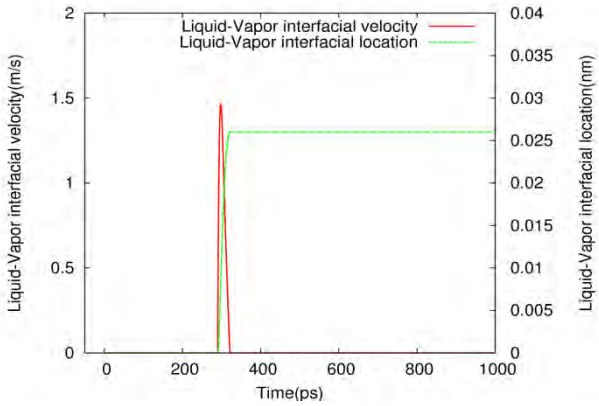

(c) Liquid-vapor interfacial velocity and location

Fig. 5 Irradiation by two consecutive 0.3 J/cm^2 laser pulses with a separation time 280 ps.

The irradiation process caused by two consecutive pulses with laser fluence 0.3 J/cm^2 and separation time ranges from 1 to 6000 ps are studied. Figure 6(a) shows the dependency of maximum melting depth on maximum temperature with different separation times. It can be seen all of the points located at upper part of the solid line, which hints two pulses will achieve a deeper melting depth with the same maximum lattice temperature. When separation time is less than 50 ps, all of these cases obtain less melting depth than others except the case with Δt = 800 ps. From Fig. 6 (b), the resolidification velocity reaches to the maximum at 800 ps. For the case with Δt = 280 ps, the melting depth is obviously increased. As shown in Fig. 6(b), at 280ps, the melting velocity becomes zero, which means that the melting depth reaches the maximum. Thus, if a deeper melting depth is desirable, the second pulse should be launched when the melting velocity becomes zero. To verify what find in Fig. 6, another case with two consecutive pulses of J = 0.35 J/cm^2 is simulated, which shows the same conclusion as discussed above. Figure 7 shows the result from this case. At 400 ps, the liquid and solid interfacial velocity reaches to zero, and the resolidification velocity reach the minimum when t = 1200 ps.

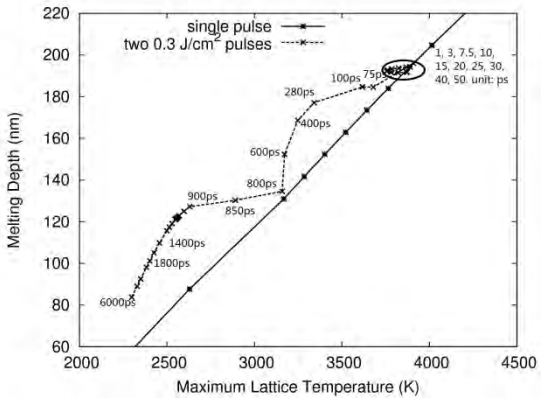

(a) Dependency of melting depth on maximum lattice temperature

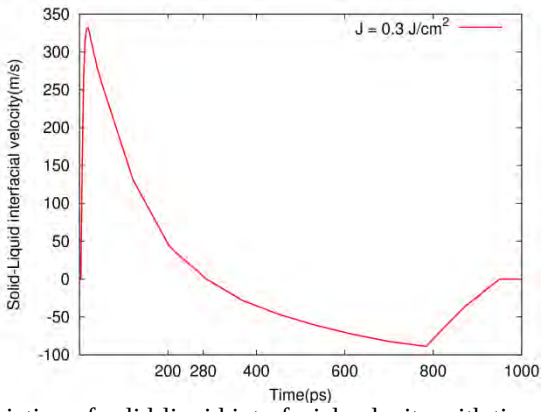

(b) Variation of solid-liquid interfacial velocity with time by a single 0.3 J/cm^2

Fig. 6 Relationship between maximum temperature and melting depth by two consecutive 0.3 J/cm^2 laser pulses with separation time ranged from 1 ps and 6000 ps.

Figure 8 shows the dependency of ablation depth caused by two 0.3 J/cm^2 pulses on maximum surface temperature. Cases with Δt ranges from 50 ps to 280 ps are obviously located above the solid line; other cases do not show an obvious increase in ablation depth. For cases with Δt equals to 10 ps, 15 ps, 20 ps, 30 ps and 40 ps, the ablation depth is slightly lower

than the corresponding single pulse. Figure 8 (b) shows that the surface temperature reaches to the first peak of 1916.73 K at around 20 ps. Thus, if deeper ablation depth is the aim of the process, the second pulse should not be launched when the surface temperature reach the peak value.

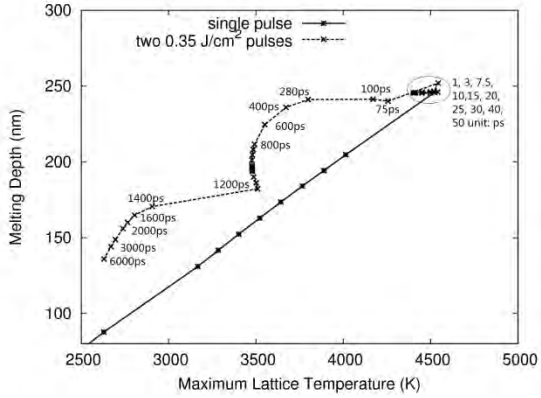

(a) Dependency of melting depth on maximum lattice temperature

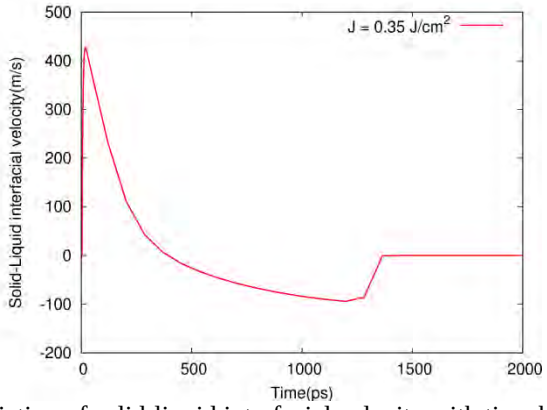

(b) Variation of solid-liquid interfacial velocity with time by a single 0.35 J/cm^2

Fig. 7 Relationship between maximum temperature and melting depth by two consecutive 0.35 J/cm^2 laser pulses with separation time ranged from 1 ps to 6000 ps.

3 Multiple pulses

Laser metal interaction with multiple pulses, which range from 2 to 10, with total laser fluence J = 0.6 J/cm^2 are studied for the following seven cases: (a) 2 pulses at 0.3 J/cm^2 per pulse, (b) 3 pulses at 0.2 J/cm^2 per pulse, (c) 4 pulses at 0.15 J/cm^2 per pulse, (d) 5 pulses at 0.12 J/cm^2 per pulse, (e) 6 pulses at 0.1 J/cm^2 per pulse, (f) 8 pulses at 0.075 J/cm^2 per pulse, (g) 10 pulses at 0.01 J/cm^2 per pulse. The separation time ranges from 1 ps to 15 ps.

The dependency of maximum temperature and melting depth on the number of pulses and separation time is shown in Figs. 9 and 10. The maximum temperature will decrease when the number of pulses increases. Correspondingly, the melting depth decreases along with the increment of the number of pulses. Figure 11 shows the comparison of melting depth, which obtained with the same maximum lattice temperature, between that from single pulse and multiple pulses with various separation times. It can be seen that all of the results from multiple pulses located at the upper part of the solid line, which means that multiple pulses are more preferable than single pulse if the aim of material processing is achieving deeper melting depth. Higher number of pulses and longer separation time will make the difference more significant.

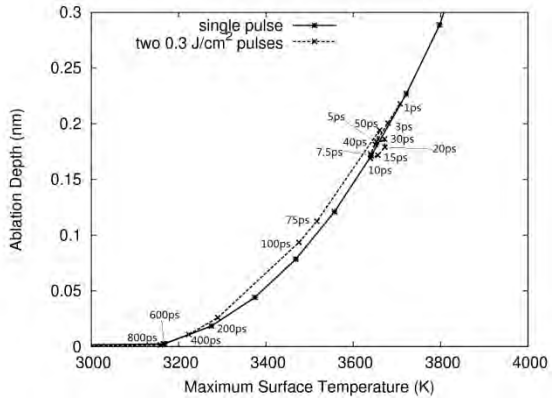

(a) Dependency of ablation depth on maximum surface temperature

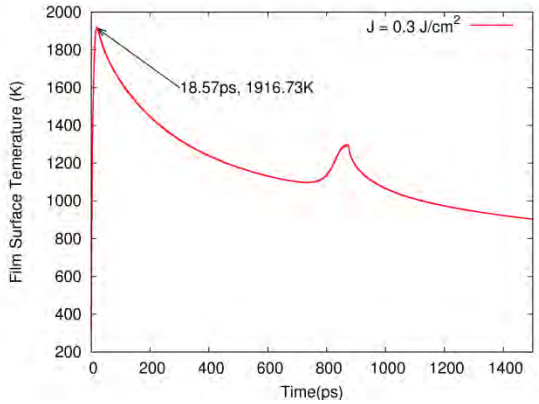

(b) Variation of surface temperature with time by a single 0.3 J/cm^2 pulse.

Fig. 8 Relationship between maximum temperature and ablation depth by two consecutive 0.3 J/cm^2 laser pulses with separation time ranged from 1 ps to 6000 ps.

Figures 12 and 13 give the relationship between number of pulses and maximum surface temperature, the relationship between number of pulses and ablation depth, respectively. It can be seen that larger number of pulse and longer separation time will lead to higher surface temperature and deeper ablation depth. Relationship between maximum surface temperature and ablation depth is shown in Fig. 14. It indicates that there is no significant difference on the ablation depth caused by the same surface temperature between single pulse irradiation and multiple pulses irradiation due to the fact that nearly all the point located on the solid line. In other words, if the aim of laser material processing is ablating material, there is no much improvement whether you chose single pulse or multiple pulse processing.

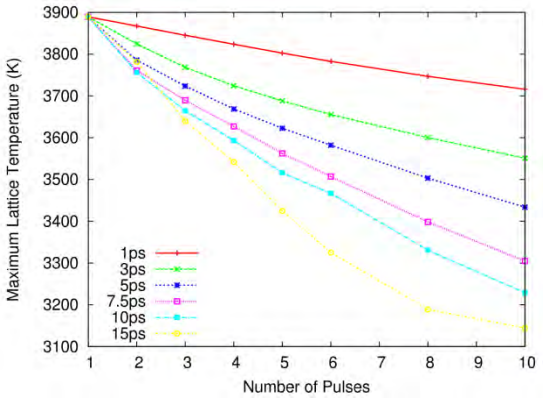

Fig. 9 Dependence of maximum temperature on pulses number and separation time.

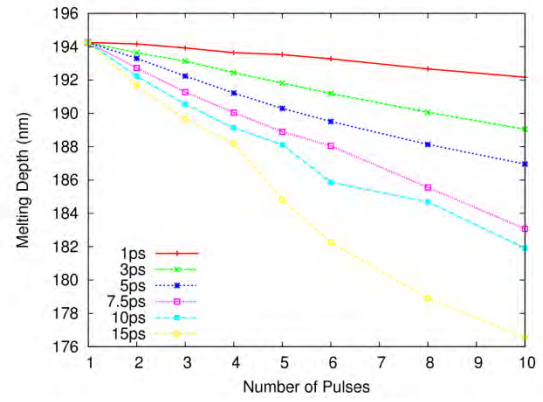

Fig. 10 Dependence of melting depth on pulses number and separation time.

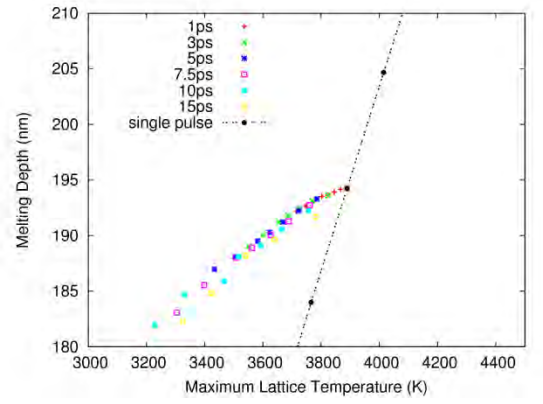

Fig. 11 Comparison of melting depth between multiple pulses irradiation and single pulse irradiation.

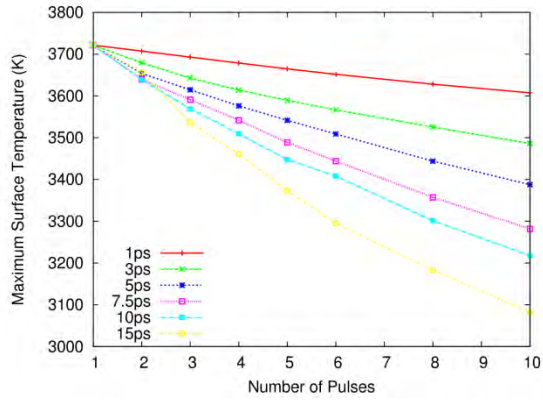

Fig. 12 Dependence of surface temperature on pulses number and separation time.

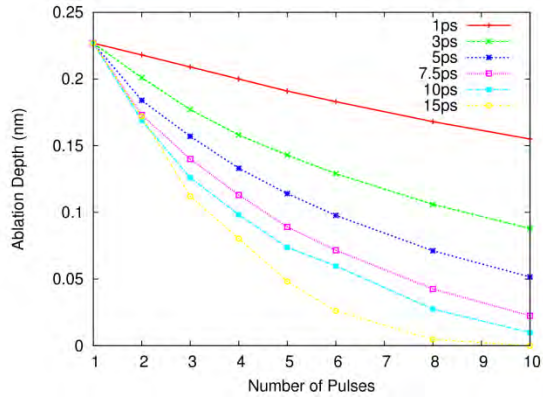

Fig. 13 Dependence of ablation depth on pulses number and separation time.

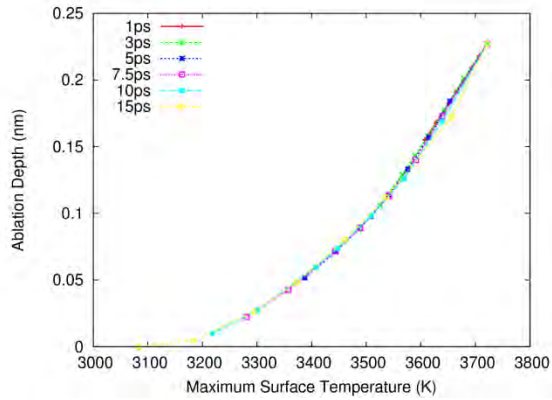

Fig. 14 Comparison of ablation depth between multiple pulses irradiation and single pulse irradiation.

Conclusions

Melting, vaporization and resolidification in a gold thin film subject to multiple femtosecond laser pulses are numerically studied in the framework of the two-temperature model. Instead of Clausius-Clapeyron equation based vaporization model, a new model which is based on wave theory is applied to capture

the vaporization process. The following conclusions can be drawn from the present study:

1 The temperature within the gold film is lower than the results obtained using the Clapeyron equation. As a result, the melting depth is slightly lower than that obtained from the Clapeyron equation under the same condition. However, the liquid-vapor interfacial velocity is two orders of magnitude higher than the old model, and the ablation depth is one order to magnitude larger than that from the old model.

2 The relationship between maximum lattice temperature and melting depth, ablation depth are analyzed and compared with that of the single pulse irradiation. For two pulses irradiation, the second pulse should be launched when the melting depth caused by the first pulse reach to the peak value. Comparing with the result from single pulse laser irradiation, two pulses will lead to higher melting depth if the maximum lattice temperature is the same.

3 For multiple laser pulses irradiation, with the same total laser fluence, larger number of pulses and longer separation times between pulses lead to smaller melting depth; in comparison with the result from single pulse which caused the same maximum lattice temperature, the melting depth is much deeper. For the purpose of ablating material, the results show no advantage in ablation with multiple pulses over single pulses.

ACKNOWLEDGMENTS

Support for this work by the U.S. National Science Foundation under Grant No. CBET-1066917 is gratefully acknowledged.

REFERENCES

[1] J. Huang, Y. Zhang, J. K. Chen, Superheating in liquid and solid phases during femtosecond-laser pulse interaction with metal film, Applied Physics A, 103, 2011, 113-121.

[2] D. Y. Tzou, A Unified Field Approach for Heat Conduction From Macro- to Micro-Scale, Journal of Heat Transfer, 117 (1, 8), 1995, 9-16.

[3] L. V. Zhigilei, P. B. S. Kodali, and B. J. Garrison, Molecular Dynamic Model for Laser Ablation and Desorption of Organic Solids, Journal of Physical Chemistry, B, 101, 1997, 2028 – 2037.

[4] C. Schäfer, and H. M. Urbassek, Metal ablation by picosecond laser pulses: A hybrid simulation, Physical Review B, 66, 2002, 115404.

[5] S. I. Anisimov, B.L. Kapeliovich, T.L. Perel'man, Electron emission from metal surface exposed to ultra-short laser pulses, Sov. Phys. JETP 39(2), 1974, 375-377.

[6] T. Q. Qiu, and C. L. Tien, Heat transfer mechanisms during short-pulse laser heating of metals, Journal of Heat Transfer – ASME, 115 (4), 1993, 835-841.

[7] D. Y. Tzou, Macro- to Microscale Heat Transfer, Taylor & Francis, Washington, DC. 1997.

[8] D. Y. Tzou, Computational techniques for microscale heat transfer, in: W. J. Minkowycz, E. M. Sparrow, J. Y. Murthy, W. J. Minkowycz, E. M. Sparrow, J. Y. Murthy (Eds.), Handbook of Numerical Heat Transfer, second ed., Wiley, Hoboken, NJ, 2006.

[9] L. Jiang, H. L. Tsai, Improved two-temperature model and its application in ultrashort laser heating of metal films, Journal of Heat Transfer, 127(10), 2005, 1167-1173.

[10] J. K. Chen, D. Y. Tzou, J. E. Beraun, A semiclassical two-temperature model for ultrafast laser heating, Internal Journal of Heat Transfer, 49 (1-2), 2006, 307-316.

[11] J. Huang, Y. Zhang, J.K. Chen, Ultrafast solid-liquid-vapor phase change in a thin gold film irradiated by multiple femtosecond laser pulses, International Journal of Heat and Mass Transfer 52, 2009, 3091-3100.

[12] F. D. Bennett, Vaporization-wave transitions, in Physics of High Energy Density, ed. By P. Caldirola, H. Knoepfel, Academic Press, New York, 1971.

[13] L. Harris, A. L. Loeb, Conductance and relaxation time of electrons in gold blacks from transmission and reflection measurements in the far infrared, Journal of the Optical Society of America. 43, 1953, 1114-1118.

[14] Ren, Y., Chen, J.K., Zhang, Y., and Huang, J., 2011, Ultrashort Laser Pulse Energy Deposition in Metal Films with Phase Changes, Applied Physics Letters, 98(19), 191105.

[15] L. S. Kuo, T. Qiu, Microscale energy transfer during picosecond laser melting of metal films, in ASME National Heat Transfer Conference, ASME, New York, 1996, 149.

[16] S. I. Anisimov, B. Rethfeld, On the theory of ultrashort laser pulse interaction with a metal, in Proceedings of SPIE – The International Society for Optical Engineering, 1997, 192.

[17] J. K. Chen, W. P. Latham, J. E. Beraun, The role of electron–phonon coupling in ultrafast laser heating, Journal of Laser Applications, 17, 2005, 63.

[18] S. S. Wellershoff, J. Hohlfeld, J. Güdde, E, and E. Matthia, The role of electron–phonon coupling in femtosecond laser damage of metal, Applied Physics A, Material Science and Process, 69, 1999, S99.

[19] P. G. Klemens, R. K. Williams, thermal conductivity of metal and alloys, International Metals Reviews, 31, 1986, 197.

[20] A. Faghri, Y. Zhang, Transport Phenomena in Multiphase Systems, Elsevier, Burlington, 2006.

[21] R. Courant, and K. O. Friedrichs, Supersonic Flow and Shock Waves, InterScience, New York, 21, 1976, 92.

[22] Y. Zhang, J. K. Chen, An Interfacial Tracking Method for ultrashort pulse laser melting and resolidification of a thin metal film, Journal of Heat Transfer, 130, 2008, 062401